Capacity per Unit Area of Distributed Antenna Systems with Centralized Processing

Laura Cottatellucci
EURECOM
Mobile Communications Department
BP193, F-06560 Sophia Antipolis, France
Email: cottatel@eurecom.fr

***Abstract*—We consider an extended wireless network with transmit and receive nodes distributed according to Bernoulli lattice processes in 1D and 2D spaces. The received signals are jointly processed at a central unit. The channel is characterized by pathloss attenuation depending on distances between transmit and receive antennas. We introduce a new class of Euclidean random matrix (ERM) to characterize the distributed antenna system (DAS). By leveraging on a suitable decomposition of these ERMs, we propose an approximated analysis of their spectra and use it to provide an analytical approximation of the capacity per unit area of the DAS.**

I. Introduction

The concept of distributed antenna systems (DAS) was introduced in [1], [2] about two decades ago. However, only recently, the wide use of remote radio heads (RRH) in 4G standards and the emerging cloud radio access network (C-RAN) architecture, which is expected to play a strategic role in 5G wireless networks, is creating the conditions to transform this concept in a mature and implementable technology. Thus, it is urgent a thorough analysis of the fundamental limits of this kind of systems. In the last decade, the study of the DAS *in downlink* has been flourishing. By modeling the location of nodes in a network as random, powerful techniques based on stochastic geometry have provided insights on capacity, connectivity, outage probability, and other fundamental aspects of the DAS downlink. An updated and detailed overview of the existing results can be found in [3]. In contrast, the study of the *DAS uplink* is limited. In [4], Gan et al. considered a DAS over a finite disc and assumed a circular layout for the system receive antennas. The capacity per user is determined by applying standard results of random matrix theory (RMT) for Wishard matrices (see e.g. [5]). The DAS uplink over a finite area with arbitrary but fixed layout for the location of transmit and receive antennas is studied in [6]. In both cases, the strong assumptions and approximations in modeling the DAS uplink yield an approximation of the DAS sum capacity coinciding with the limiting capacity of a standard multiuser multiple input multiple output (MIMO) system with co-located antennas. As consequence of this approximation, the sum capacity obtained by numerical simulations and the analytical results match well only in the cases when the receive antenna layout has a negligible effect on the DAS uplink sum capacity, as noticed in [7]. In [7], Dai considered transmit and receive antennas homogeneously distributed within a given finite cell and centralized processing of all the received signals. Lower bounds of DAS uplink capacity are derived under the assumption of channel state information (CSI) at the receiver and with or without CSI at the transmitters. Power control is performed such that all the transmit signals are received with constant total power.

A related research field focuses on multicell networks with regular layouts and joint processing of all received signals. The so-called Wyner model, a one dimensional infinite linear network with base stations regularly spaced and jointly processed signals, is adopted and the analysis is based on RMT. An asymptotic analysis of CDMA networks with spreading factor and number of users per cell scaling with constant ratio is proposed in [8]. Independently of the transmitters' locations, the signals are received at a reference power at their cell base station (BS) and are attenuated by a unique parameter $\alpha < 1$ at the two adjacent BSs. In [9], a similar asymptotic analysis is carried out for a multi-cell MIMO Wyner network with the number antennas at each BS and users per cell scaling at a constant ratio. More recently, a more complex model with directional antennas, finite number of users and cooperating cells was considered in [10]. Although the analysis based on RMT can be really insightful, the above mentioned existing models do not capture the impact of the geographical random distributions of transmit and receive antennas. Coherent potential approximation, a technique developed in statistical mechanics, is applied in [11] to study a two-dimensional network with transmitters and receivers randomly distributed over a lattice.

In [12], we extended the class of Euclidean random matrices (ERM), introduced and defined by Mézard et al. in [13] for a single set of random nodes to two independent random sets. Then, we proposed an application of this new class of random matrices to the study of the DAS uplink capacity with transmit and receive nodes randomly distributed according to two independent Bernoulli lattice processes with given intensities. By leveraging on the initial mathematical framework sketched in [12], in this paper, we present a detailed analysis of the DAS uplink capacity under the assumption of constant transmit power, knowledge of CSI at the centralized processing unit and no CSI at the transmitters. Inspired by a decomposition adopted in [14] and based on a set of eigenfunctions, we adopt an orthogonal vector basis yielding a decomposition of ERM into a deterministic kernel and two random matrices. Based on this decomposition, we discuss an analysis of the eigenvalue spectrum based on the eigenvalue moments. Additionally, we approximate the random matrix elements of the decomposition by classes of free matrices. This approximation enables the ap-

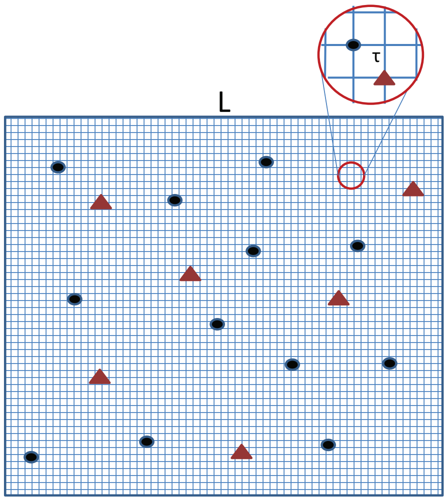

Fig. 1. Representation of $\mathcal{A}_L^\sharp$. The large squared box represents the network surface. The intersection points of the grid correspond to the points of the lattice. Triangles and circles represent realizations of the homogeneous Bernoulli processes of transmit and receive antennas, respectively.

plication of powerful tools of free probability [15]. It is worth noticing that this approximation has been successfully applied both in physics (e.g. [14], [16]) and telecommunications (e.g. [17]). We utilize the approximation of the eigenvalue distribution to determine an analytical approximation of the capacity per unit area of extended networks with randomly distributed transmitters and receivers with centralized processing. The eigenvalue moments are essential for the performance analysis of a large class of linear receivers [18].

II. System Model

We adopt the same system model and notation adopted in [12] and we describe them in this section to keep the paper self-contained. Throughout this paper, we will consider both networks over 1-dimensional (1D) and 2-dimensional (2D) spaces. The corresponding models and notation are discussed in parallel. Let $\mathcal{A}_L = \left[-\frac{L}{2}, +\frac{L}{2}\right) \times \left[-\frac{L}{2}, +\frac{L}{2}\right)$ be a squared box of side L and area $A = L^2$ in $\mathbb{R}^2$ and $\widetilde{\mathcal{A}}_L = \left[-\frac{L}{2}, +\frac{L}{2}\right)$ a segment of length L in $\mathbb{R}$. Additionally, let $\tau > 0$ be a real such that $L = \tau\theta$, with θ positive integer, and let $\mathbf{w} \equiv (\tau(\overline{w}_x + 1/2), \tau(\overline{w}_y + 1/2))$ or $w = \tau(\overline{w}_x + 1/2)$, with $\overline{w}_x, \overline{w}_y \in \mathbb{Z}$, be points of a regular lattice in $\mathbb{R}^2$ or $\mathbb{R}$, respectively. To easy the notation, in the following, without loss of generality (l.o.g.) we assume θ even and denote by $\mathcal{A}_L^\sharp$ ($\widetilde{\mathcal{A}}_L^\sharp$) the set of lattice points in $\mathcal{A}_L$ ($\widetilde{\mathcal{A}}_L$), i.e. $\mathcal{A}_L^\sharp \equiv \{\mathbf{w} | \, \mathbf{w} \in \mathcal{A}_L, \overline{w}_x, \overline{w}_y = -\frac{\theta}{2}, -\frac{\theta}{2} + 1, \ldots \frac{\theta}{2} - 1\}$ ($\widetilde{\mathcal{A}}_L^\sharp \equiv \{w | \, w \in \widetilde{\mathcal{A}}_L, \overline{w}_x = -\frac{\theta}{2}, -\frac{\theta}{2} + 1, \ldots \frac{\theta}{2} - 1\}$). The set $\mathcal{A}_L^\sharp$ is shown in Fig. 1. Both transmit and receive nodes are independently and homogeneously distributed over the squared grid $\mathcal{A}_L^\sharp$. More specifically, the distributed transmit and receive antennas in $\mathbb{R}^2$ are modeled as homogeneous Bernoulli lattice processes $\Phi^{\mathcal{T}}_{\mathcal{A}_L^\sharp}$ and $\Phi^{\mathcal{R}}_{\mathcal{A}_L^\sharp}$ with parameters $\gamma_T = \rho_T \tau^2$ and $\gamma_R = \rho_R \tau^2$, respectively[1]. We denote by $\mathcal{T} = \{\mathbf{t}_j\}$ and $\mathcal{R} = \{\mathbf{r}_i\}$ the realizations of the two Bernoulli lattice processes with cardinality N_T and N_R, respectively. Additionally, $\mathbf{t}_j = (t_{x,j}, t_{y,j})$ and $\mathbf{r}_i = (r_{x,i}, r_{y,i})$ correspond to the Euclidean coordinates of transmitter j and receiver i in $\mathcal{A}_L^\sharp$. In Fig. 1, triangles and circles represent the realizations $\mathcal{T}$ and $\mathcal{R}$, respectively. Similarly, in $\mathbb{R}$, the two Bernoulli lattice points $\Phi^{\widetilde{\mathcal{T}}}_{\widetilde{\mathcal{A}}^\sharp}$ and $\Phi^{\widetilde{\mathcal{R}}}_{\widetilde{\mathcal{A}}^\sharp}$ are characterized by the parameters $\widetilde{\gamma}_T = \widetilde{\rho}_T \tau$ and $\widetilde{\gamma}_R = \widetilde{\rho}_R \tau$ and the realizations of the transmit and receive node processes are denoted by $\widetilde{\mathcal{T}}$ and $\widetilde{\mathcal{R}}$, respectively.

Transmit and receive antennas are in line of sight and a channel coefficient between a transmit-receive antenna pair, up to a phase rotation, depends on the pathloss attenuation and it is given by

$$f(\mathbf{r}_i, \mathbf{t}_j) = f(\|\mathbf{r}_i - \mathbf{t}_j\|_2) \tag{1}$$

where $\|\mathbf{r}_i - \mathbf{t}_j\|_2$ denotes the Euclidean distance between transmit antenna j and receive antenna i. In order to keep the presentation insightful and the computation simple, we follow the approach in [20] and model a channel coefficient as an exponentially decaying function of the two antenna distance

$$f(\mathbf{r}_i, \mathbf{t}_j) = \mathrm{e}^{-k_0 \|\mathbf{r}_i - \mathbf{t}_j\|_2} \tag{2}$$

where $k_0 > 0$ is a positive constant.

Remark 1

- *As pointed out in [21], without loss of conceptual scope, we focus on real valued channels and neglect the effects of phase rotations.*
- *In theoretical analysis it is often adopted the function*[2] $f(\mathbf{r}_i, \mathbf{t}_j) = \|\mathbf{r}_i - \mathbf{t}_j\|_2^{-\alpha}$ *where* $\alpha \in [1, 2]$. *However, this function presents a vertical asymptote for a distance equal to zero and it needs to be further modified to be realistic at short distances.*
- *For the applicability of the mathematical tools proposed in the following section,* $f(\cdot,\cdot)$ *is required to vanish at the boundary of a finite disc (assumption satisfied in physical systems) and to satisfy the conditions of existence of a Fourier transform.*

We further assume that the receive antennas are connected to a processing unit such that decoding is performed jointly. The transmit nodes do not have knowledge of the channel and transmit at the same power P. The receivers are impaired by additive white Gaussian noise with variance σ^2. Then, the signal received at the discrete time instant t by receiver i is given by

$$y_i(t) = \sum_j \sqrt{P} f(\|\mathbf{r}_i - \mathbf{t}_j\|_2) x_j(t) + w_i(t) \tag{3}$$

where $x_j(t)$ is the unitary energy symbol transmitted by node j and $w_i(t)$ is the additive white Gaussian noise at receive node i.

[1] When we consider two sequences of denser and denser Bernoulli lattice processes with constant intensity ρ_T and ρ_R and $\tau \to 0$, the two sequences of processes converge in distribution to limiting Poisson point processes [19] with the same intensity ρ_T and ρ_R.

[2] The square of this channel coefficient coincides with the well-known expression for the pathloss attenuation.

Then, at the central processing unit $\mathbf{y}(t)$, the received signal vector is given by

$$\mathbf{y}(t) = \sqrt{P}\mathbf{F}^{(L)}\mathbf{x}(t) + \mathbf{w}(t), \quad (4)$$

where $\mathbf{x}(t) = (x_1(t), x_2(t), \dots x_{N_T}(t))^T$, $\mathbf{F}^{(L)}$ is an $N_R \times N_T$ random matrix whose (i,j) element is the value of a deterministic function $f(\mathbf{r}_i, \mathbf{t}_j)$ in $\mathcal{A}_L^\sharp \times \mathcal{A}_L^\sharp$ depending on the random antenna locations $\mathbf{r}_i, \mathbf{t}_j$ (r_i, t_j) for the 2D-system and $\mathbf{w}(t) = (w_1(t), w_2(t), \dots w_{N_T}(t))^T$. In the following, without ambiguity we can omit the time interval t. Similarly, for 1D-systems, channel coeffcients are given by the function $\widetilde{f}(r_i, t_j) = \mathrm{e}^{-k_0|r_i - t_j|}$. For the system model, the matrix $\mathbf{F}^{(L)}$ in (4) is replaced by a matrix $\widetilde{\mathbf{F}}^{(L)}$ with (i,j)-element equal to $\widetilde{f}(r_i, t_j)$.

III. Spectral Analysis of a Class of ERM

As well known (see e.g. [22], [23]), the fundamental limits of the vector channel system in (4) depends on the eigenvalue spectrum of the matrix $\mathbf{F}^{(L)}$. In this section we follow the approach of decomposing the ERM $\mathbf{F}^{(L)}$ in the product of a deterministic matrix capturing the complexity of the function $f(\cdot,\cdot)$ and two independent random matrices as proposed in [12]. This decomposition was inspired by a similar decomposition proposed in [14]. The fundamental differences compared to the work in [14] are the following. In [14] an infinite set of continuous eigenfunctions was proposed. However, it was completely unclear how to associate sequences of finite matrices scaling with constant ratio to this set. Instead, in [12] and here we propose a decomposition based on finite set of orthogonal vectors whose dimension scales with L. A second difference compared to the approach in [14] lies in the fact that here we consider a new class of ERM with two independent sets of random nodes instead of the usual ERM class introduced in [13]. Finally, the exponential functions $f(\cdot,\cdot)$ considered here have properties substantially different from the sinusoidal functions considered in [14].

In order to introduce the set of orthogonal vectors, we define the set of points $\mathcal{L}_\pi^\sharp \equiv \left\{\boldsymbol{\omega} = \left(\frac{2\pi\ell_x}{\theta}, \frac{2\pi\ell_y}{\theta}\right) \middle| \, \ell_x, \ell_y = \{-\frac{\theta}{2}, \dots 0, +1 \dots + \frac{\theta}{2} - 1\right\}$ and define the set of orthogonal functions on the discrete and finite set $\mathcal{A}_L^\sharp$

$$\left\{\psi_{\boldsymbol{\omega}}^{(L)}(\mathbf{w}) \middle| \psi_{\boldsymbol{\omega}}^{(L)}(\mathbf{w}) = \frac{1}{\theta}\exp\left(\frac{+i\boldsymbol{\omega}\mathbf{w}}{\tau}\right), \right.$$
$$\left. \boldsymbol{\omega} \in \mathcal{L}_\pi^\# \setminus \{\mathbf{0}\} \text{ and } \boldsymbol{\omega} \in \mathcal{A}_L^\sharp \right\}. \quad (5)$$

Similarly, for the 1D-system, defined the set $\widetilde{\mathcal{L}}_\pi^\sharp \equiv \left\{\omega = \frac{2\pi\ell_x}{\theta} \middle| \, \ell_x = \{-\frac{\theta}{2}, \dots 0, +1 \dots + \frac{\theta}{2} - 1\right\}$ and we adopt the set of orthogonal functions on $\widetilde{\mathcal{A}}_L^\sharp$

$$\left\{\widetilde{\psi}_\omega^{(L)}(w) \middle| \widetilde{\psi}_\omega^{(L)}(w) = \frac{1}{\sqrt{\theta}}\exp\left(\frac{+i\omega w}{\tau}\right), \right.$$
$$\left. \omega \in \widetilde{\mathcal{L}}_\pi^\# \setminus \{0\} \text{ and } \omega \in \widetilde{\mathcal{A}}_L^\sharp \right\}. \quad (6)$$

The interested reader is referred to [12] for a discussion on the properties of (5) and (6). Then, as in [12], for the 2D-system, we define the discrete transform

$$T_{\boldsymbol{\omega},\boldsymbol{\nu}}^{(L)} = \sum_{\mathbf{r}\in\mathcal{A}_L^\sharp} \sum_{\mathbf{t}\in\mathcal{A}_L^\sharp} f(\mathbf{r}, \mathbf{t})\psi_{\boldsymbol{\omega}}^{(L)*}(\mathbf{r})\psi_{\boldsymbol{\nu}}^{(L)}(\mathbf{t})$$

and its inverse

$$f(\mathbf{r}, \mathbf{t}) = \sum_{\boldsymbol{\omega},\boldsymbol{\nu}\in\mathcal{L}_\pi^\#\setminus\{\mathbf{0}\}} T_{\boldsymbol{\omega},\boldsymbol{\nu}}^{(L)}\psi_{\boldsymbol{\omega}}^{(L)}(\mathbf{r})\psi_{\boldsymbol{\nu}}^{(L)*}(\mathbf{t}) \quad (7)$$

being $\cdot^*$ the complex conjugate operator. Similar relations holds for the function $\widetilde{f}(r_i, t_j)$ and are omitted here for conciseness.

As straightforward consequence of (7), the matrix $\mathbf{F}^{(L)}$ can be written as

$$\mathbf{F}^{(L)} = \boldsymbol{\Psi}_R^{(L)}\mathbf{T}^{(L)}\boldsymbol{\Psi}_T^{(L)H} \quad (8)$$

where $\mathbf{T}^{(L)}$ is a $(\theta^2 - 1) \times (\theta^2 - 1)$ matrix with elements $T_{\boldsymbol{\omega},\boldsymbol{\nu}}^{(L)}$, $\boldsymbol{\Psi}_R^{(L)}$ is an $N_R \times (\theta^2 - 1)$ matrix with element $(j, \boldsymbol{\omega})$ $\psi_{j,\boldsymbol{\omega}}^{(L)} = \psi_{\boldsymbol{\omega}}^{(L)}(\mathbf{r}_j)$ and $\boldsymbol{\Psi}_T^{(L)}$ is an $N_T \times (\theta^2 - 1)$ matrix with element $(k, \boldsymbol{\nu})$ $\psi_{k,\boldsymbol{\nu}}^{(L)} = \psi_{\boldsymbol{\nu}}^{(L)}(\mathbf{t}_k)$. Let us observe that we index the elements of the matrices $\mathbf{T}^{(L)}$, $\boldsymbol{\Psi}_R^{(L)}$, and $\boldsymbol{\Psi}_T^{(L)}$ along the dimensions of size $\theta^2 - 1$ by $\boldsymbol{\omega}, \boldsymbol{\nu} \in \mathcal{L}_\pi^\# \setminus \{\mathbf{0}\}$ instead of the usual indexing by natural numbers. Here, the underlying assumption is that the 2-dimensional vectors in $\mathcal{L}_\pi^\# \setminus \{\mathbf{0}\}$ are mapped according to an arbitrary mapping criterion onto the set of natural numbers $\{0, 1, \dots \theta^2 - 1\}$. The matrices $\mathbf{T}^{(L)}$, $\boldsymbol{\Psi}_R^{(L)}$, and $\boldsymbol{\Psi}_T^{(L)}$ are built according to this mapping. However, their elements are indexed according to the inverse mapping from $\{0, 1, \dots \theta^2 - 1\}$ in $\mathcal{L}_\pi^\# \setminus \{\mathbf{0}\}$ since the mapping criterion is irrelevant for further studies while the values of the vectors $\boldsymbol{\omega}, \boldsymbol{\nu}$ play a key role.

When the area of $\mathcal{A}^{(L)}$ increases θ, N_R and N_T also increases according to the following relations

$$\frac{N_R}{\theta^2} \to \rho_R\tau^2, \qquad \frac{N_T}{\theta^2} \to \rho_T\tau^2, \qquad \frac{N_R}{N_T} \to \frac{\rho_R}{\rho_T}, \quad (9)$$

and the sizes of the matrices $\boldsymbol{\Psi}_R^{(L)}$, $\mathbf{T}^{(L)}$, and $\boldsymbol{\Psi}_T^{(L)}$ increase with ratios converging to a constant as typical in random matrix theory. Shortly, we denote the growing of the area network and the corresponding network nodes according to (9) by $L \to +\infty$.

For 1D-systems, the decomposition $\widetilde{\mathbf{F}}^{(L)} = \widetilde{\boldsymbol{\Psi}}_R^{(L)}\widetilde{\mathbf{T}}^{(L)}\widetilde{\boldsymbol{\Psi}}_T^{(L)H}$ holds with obvious meaning for the $(\theta - 1) \times (\theta - 1)$ matrix $\widetilde{\mathbf{T}}^{(L)}$, the $N_R \times (\theta - 1)$ matrix $\widetilde{\boldsymbol{\Psi}}_R^{(L)}$, and the $N_T \times (\theta - 1)$ matrix $\widetilde{\boldsymbol{\Psi}}_T^{(L)}$.

In order to analyze the eigenvalue spectrum of the matrix $\widetilde{\mathbf{C}}^{(L)} = \widetilde{\mathbf{F}}^{(L)H}\widetilde{\mathbf{F}}^{(L)}$ and $\mathbf{C}^{(L)} = \mathbf{F}^{(L)H}\mathbf{F}^{(L)}$ as $L \to +\infty$, it is essential to characterize the matrices $\widetilde{\mathbf{T}}^{(L)}$ and $\mathbf{T}^{(L)}$ as $L \to +\infty$ and determine their asymptotic eigenvalue distribution.

The matrix $\widetilde{\mathbf{T}}^{(L)}$ can be written in closed form and it is described in the following lemma.

Lemma 1 *Define* $\nu = \dfrac{2\pi\ell}{\theta}$. *The diagonal and the out-diagonal elements of the matrix* $\widetilde{\mathbf{T}}^{(L)}$, $\widetilde{T}_{\ell,\ell}^{(L)}$ *and* $\widetilde{T}_{\ell,m}^{(L)}$ *are shown in (10) and (11) at the top of next page, respectively.*

$$\widetilde{T}_{\ell,\ell}^{(L)} = 1 - \frac{2(\mathrm{e}^{-k_0\tau(\theta-1)}(\mathrm{e}^{k_0\tau} - \cos(\nu)) - \mathrm{e}^{k_0\tau}\cos(\nu) + 1)}{\mathrm{e}^{2k_0\tau} - 2\mathrm{e}^{k_0\tau}\cos(\nu) + 1} + \frac{2\mathrm{e}^{k_0\tau}(2\mathrm{e}^{k_0\tau} - \cos(\nu) - \mathrm{e}^{2k_0\tau}\cos(\nu))}{\theta(\mathrm{e}^{2k_0\tau} - 2\mathrm{e}^{k_0\tau}\cos(\nu) + 1)^2} + \frac{2\mathrm{e}^{-k_0\tau(\theta-1)}(\mathrm{e}^{k_0\tau} - \cos(\nu))}{(\mathrm{e}^{2k_0\tau} - 2\mathrm{e}^{k_0\tau}\cos(\nu) + 1)} + \frac{2\mathrm{e}^{-k_0\tau(\theta-1)}(\mathrm{e}^{2k_0\tau}\cos(\nu) - 2\mathrm{e}^{k_0\tau} + \cos(\nu))}{\theta(\mathrm{e}^{2k_0\tau} - 2\mathrm{e}^{k_0\tau}\cos(\nu) + 1)^2} \tag{10}$$

$$\widetilde{T}_{\ell,m}^{(L)} = \frac{\cos(\pi m)\cos(\pi\ell)\cos(\pi(\ell-m)/\theta)(1-\mathrm{e}^{-k_0\tau\theta})(4\cos(\pi(\ell-m)/\theta) - 2(\mathrm{e}^{k_0\tau} + \mathrm{e}^{-k_0\tau})\cos(\pi(\ell+m)/\theta))}{\theta\left((2\cos(\pi(\ell-m)/\theta) - (\mathrm{e}^{k_0\tau} + \mathrm{e}^{-k_0\tau})\cos(\pi(\ell+m)/\theta))^2 + (\mathrm{e}^{-k_0\tau} - \mathrm{e}^{k_0\tau})^2\sin(\pi(\ell+m)/\theta)^2\right)} \tag{11}$$

For $\theta \to \infty$, $\widetilde{T}_{\ell,m}^{(L)} \to 0$ with rate θ^{-1} while the diagonal elements converge to

$$\widetilde{T}_{\ell,\ell}^{(L)} \stackrel{\theta\to+\infty}{\to} \widetilde{T}_{\nu}^{\infty} = \frac{\mathrm{e}^{2k_0\tau} - 1}{\mathrm{e}^{2k_0\tau} - 2\mathrm{e}^{k_0\tau}\cos\nu - 1}. \tag{12}$$

Although it is not proven (see [12] for discussions) that the asymptotic eigenvalue spectrum for $\theta \to +\infty$ coincides with the diagonal elements $\widetilde{T}_{\nu}^{\infty}$, numerous simulations support this conjecture.

CONJECTURE 1 *As $\theta \to +\infty$ the eigenvalues of the matrix $\widetilde{\mathbf{T}}^{(L)}$ converges to $\widetilde{T}_{\nu}^{\infty}$ in (12) with $\nu \in [-\pi, \pi)$ and the eigenvalue probability density function (pdf) converges to the following function*

$$f_{\widetilde{\mathbf{T}}}(x) = \frac{e^{k_0\tau} - e^{-k_0\tau}}{2\pi x\sqrt{(x_{\max} - x)(x - x_{\min})}} \tag{13}$$

with support $[x_{\min}, x_{\max}]$ and $x_{\min} = \dfrac{e^{k_0\tau} - 1}{e^{k_0\tau} + 1}$ and $x_{\max} = \dfrac{e^{k_0\tau} + 1}{e^{k_0\tau} - 1}$.

The pdf $f_{\widetilde{\mathbf{T}}}(x)$ can be derived from the expression of $\widetilde{T}_{\nu}^{\infty}$ by use of the standard definition of pdf.

For $2D$-system, it is not possible to find a closed form expression for the elements of the finite matrix $\mathbf{T}^{(L)}$. We conjecture that also for $\mathbf{T}^{(L)}$, the asymptotic eigenvalues coincide with the asymptotic diagonal elements of the matrix and use fundamental properties of the Fourier transform to determine the asymptotic values of the diagonal elements of $\mathbf{T}^{(L)}$.

LEMMA 2 *[12] Let $\epsilon > 0$ be an arbitrary small positive value and let $\tau \le \frac{\pi^2\epsilon}{2k_0}$. Then, up to negligible aliasing effects, as $L \to +\infty$, the diagonal elements of matrix $\mathbf{T}^{(L)}$ converges to finite values given by*

$$T_{\boldsymbol{\ell},\boldsymbol{\ell}}^{(L)} \stackrel{\theta\to+\infty}{\to} T(\boldsymbol{\omega}) = \frac{2\pi k_0\tau}{\left(\sqrt{\tau^2k_0^2 + \omega_x^2 + \omega_y^2}\right)^3}$$

where $\boldsymbol{\omega} = \left(\frac{2\pi\ell_x}{\theta}, \frac{2\pi\ell_y}{\theta}\right) \in \mathcal{L}_\pi \equiv [-\pi,\pi] \times [-\pi,\pi]$.

Then, by conjecturing that asymptotically the eigenvalues coincides with the asymptotic limits of the diagonal elements we state the following.

CONJECTURE 2 *Let $\epsilon > 0$ be an arbitrary small positive value and let $\tau \le \frac{\pi^2\epsilon}{2k_0}$. Then, the asymptotic eigenvalue density function of matrix $\mathbf{T}^{(L)}$ as $L \to +\infty$ is given by*

$$f_{\mathbf{T}}(x) = \frac{(2\pi k_0\tau)^{2/3}}{6\pi}x^{-5/3}, \qquad \frac{2\pi k_0\tau}{(\sqrt{k_0^2\tau^2 + \pi^2})^3} \le x \le \frac{2\pi}{k_0^2\tau^2}$$

and can be effectively approximated elsewhere by $f_{\mathbf{T}} = \left(1 - \frac{\pi}{4}\right)\delta(x - \eta)$ where η is a positive constant in the interval[3] $\left[\frac{2\pi k_0\tau}{(\sqrt{k_0^2\tau^2 + 2\pi^2})^3}, \frac{2\pi k_0\tau}{(\sqrt{k_0^2\tau^2 + \pi^2})^3}\right]$.

By applying the same approximation to the 1D-system we can state as follows.

LEMMA 3 *Let $\epsilon > 0$ be an arbitrary small positive value and let $\tau \le \frac{\pi\epsilon}{2k_0}$. Then, up to negligible aliasing effects, as $L \to +\infty$, the diagonal elements of matrix $\widetilde{\mathbf{T}}^{(L)}$ converges to finite values given by*

$$\widetilde{T}(\omega) = \frac{2k_0\tau}{k_0^2\tau^2 + \omega^2} \qquad \text{for } |\omega| \le \pi. \tag{14}$$

The derivation of this lemma follows along the same line of the derivation of Lemma 2 sketched in [12].

We are interested in characterizing the spectrum of the matrices $\mathbf{C}^{(L)}$ and $\widetilde{\mathbf{C}}^{(L)}$, as R, T, $\theta^2 \to \infty$ with constant ratio, in terms of their eigenvalue moments, i.e. $m_{\mathbf{C}}^{(n)} = \mathrm{E}\{\mathrm{tr}\mathbf{C}^n\}$ and $m_{\widetilde{\mathbf{C}}}^{(n)} = \mathrm{E}\left\{\mathrm{tr}\widetilde{\mathbf{C}}^n\right\}$, where the expectation are w.r.t. the corresponding Bernoulli processes and $\mathrm{tr}(\cdot)$ denotes the trace of the squared matrix argument normalized to the matrix dimension, e.g. $\mathrm{tr}(\mathbf{C}^n) = \frac{1}{N_T}\mathrm{Trace}(\mathbf{C}^n)$. To make the problem analytically tractable we approximate their asymptotic eigenvalues moments by the asymptotic eigenvalues moments of the matrices $\mathbf{C}_d^{(L)}$ and $\widetilde{\mathbf{C}}_d^{(L)}$, differing from the matrices $\mathbf{C}^{(L)}$ and $\widetilde{\mathbf{C}}^{(L)}$ since that matrices $\mathbf{T}^{(L)}$ and $\widetilde{\mathbf{T}}^{(L)}$ are replaced by the matrices $\mathbf{T}_d^{(L)}$ and $\widetilde{\mathbf{T}}_d^{(L)}$ obtained from the original matrices by suppressing the out-diagonal elements which are asymptotically vanishing. Then, the following propositions holds.

PROPOSITION 1 *Let $m_{\mathbf{T}}^{(n)} = \int_0^\infty x^n f_{\mathbf{T}}(x)\mathrm{d}x$ be the n-order eigenvalue moment of the matrix $\mathbf{T}^{(L)}$ as $L \to +\infty$. Then,*

$$m_{\mathbf{T}}^{(2)} = \frac{\pi^3}{k_0^2}\frac{(2k_0^2\tau^2 + \pi^2)}{(k_0^2\tau^2 + \pi^2)^2}$$

[3] Because of the constraints on τ for ϵ arbitrarily small also the values on this interval are close to zero.

and

$$m_{\mathbf{T}}^{(4)} = \frac{(k_0^2\tau^2+\pi^2)^{17/2} - k_0^{17}\tau^{17}}{58752\pi^7 k_0^3\tau^3}.$$

As $\theta^2, N_T, N_R \to \infty$ with constant ratios $\rho_T\tau^2$ and $\rho_R\tau^2$, the first asymptotic eigenvalue moment of the matrix $\mathbf{C}_d^{(L)}$ converges to the value

$$m_{\mathbf{C}_d}^{(1)} \to \rho_R\tau^2 m_{\mathbf{T}}^{(2)}$$

and the second order moment converges to

$$m_{\mathbf{C}_d}^{(2)} \to \rho_T\rho_R^2\tau^6 m_{\mathbf{T}}^{(4)} + \rho_R(\rho_T+\rho_R)\tau^4(m_{\mathbf{T}}^{(2)})^2 + \frac{\rho_R\tau^2}{(2\pi)^6}$$
$$\int_{\mathcal{D}_1} T(\boldsymbol{\omega}_1)\mathrm{d}\boldsymbol{\omega}_1 \int_{\mathcal{D}_2} T(\boldsymbol{\omega}_2)\mathrm{d}\boldsymbol{\omega}_2 \int_{\mathcal{D}_3} T(\boldsymbol{\omega}_3)T(\boldsymbol{\omega}_1+\boldsymbol{\omega}_2-\boldsymbol{\omega}_3)\mathrm{d}\boldsymbol{\omega}_3$$

where $\mathcal{D}_1 = \mathcal{D}_2 = [-\pi, +\pi]^2$ and $\mathcal{D}_3 = [-\pi,\, \omega_{x_1}+\omega_{x_2}+\pi]\times[-\pi,\, \omega_{y_1}+\omega_{y_2}+\pi]$

REMARK 2 *Note that $m_{\mathbf{C}_d}^{(2)}$ cannot be expressed in terms of $m_{\mathbf{T}}^{(n)}$, the eigenvalue moments of the deterministic matrix $\mathbf{T}^{(L)}$. A complex convolution of the two dimensional function $T(\boldsymbol{\omega})$ need be computed and implies the computation of an integral in a 6-dimensional space, which is practically unfeasible. This discourages a combinatorial analysis to find a general expression for the eigenvalue moments of any order n.*

The analysis simplifies for the 1D-system as follows.

PROPOSITION 2 *The first two eigenvalue moments of the matrix $\widetilde{\mathbf{C}}_d^{(L)}$ converge to*

$$m_{\widetilde{\mathbf{C}}_d}^{(1)} \to \widetilde{\rho}_R\tau m_{\widetilde{\mathbf{T}}}^{(2)},$$

$$m_{\widetilde{\mathbf{C}}_d}^{(2)} \to \widetilde{\rho}_T\widetilde{\rho}_R^2\tau^3 m_{\widetilde{\mathbf{T}}_d}^{(4)} + \widetilde{\rho}_R(\widetilde{\rho}_T+\widetilde{\rho}_R)\tau^2(m_{\widetilde{\mathbf{T}}_d}^{(2)})^2 + $$
$$+\frac{\widetilde{\rho}_R\tau}{(2\pi)^3}\int_{-\pi}^{\pi}\widetilde{T}(\omega_1)\mathrm{d}\omega_1\int_{-\pi}^{+\pi}\widetilde{T}(\omega_2)\mathrm{d}\omega_2\cdot$$
$$\cdot\int_{-\pi}^{\omega_1+\omega_2+\pi}\widetilde{T}(\omega_3)\widetilde{T}(\omega_1+\omega_2-\omega_3)\mathrm{d}\omega_3$$

with $m_{\widetilde{\mathbf{T}}}^{(n)} = \frac{1}{2\pi}\int_{-\pi}^{\pi}\widetilde{T}^n(\omega)\mathrm{d}\omega$.

The proofs of Proposition 1 and 2 follow from lengthly combinatorial arguments along the same line as the results in [24]. Due to space constraints we omit the details of the proof.

REMARK 3 *Let us observe that the independent random matrices $\widetilde{\mathbf{\Psi}}_R^{(L)}$ and $\widetilde{\mathbf{\Psi}}_T^{(L)}$ for a 1D-system are random Vandermonde matrices with entries in the unit circle (up to a cyclic column rotation). In [24], the eigenvalue moments of matrices of the type $\prod_i \mathbf{D}_i\mathbf{V}_i^H\mathbf{V}_i$, being $\mathbf{D}_i$ diagonal deterministic matrices and $\mathbf{V}_i$ random Vandermonde matrices, have been studied. However, the theory developed in [24] is not applicable to the analysis of these Euclidean matrices since an Euclidean matrix is approximated by a product of the type $\mathbf{D}\mathbf{V}_1\mathbf{V}_1^H\mathbf{D}\mathbf{V}_2\mathbf{V}_2^H$ and its powers. The effect of the matrices $\mathbf{V}_i\mathbf{V}_i^H$ on the asymptotic behaviour of the global product differs substantially from the one of the matrices $\mathbf{V}_i^H\mathbf{V}_i$ as apparent when we consider that the eigenvalue moments in [24] can be expressed in terms of the eigenvalue moments of the deterministic matrix while in the Euclidean case complex convolutions of the diagonal matrix are required.*

Additionally, let us assume that the j-th element of the Bernoulli process $\Phi_{\widetilde{\mathcal{A}}_L^\#}$ is kept fixed, i.e. we consider the Bernoulli process conditioned to $t_j = \overline{t}$ and denote it by $\Phi_{\widetilde{\mathcal{A}}_L^\#}^{\widetilde{\mathcal{T}}}|t_j = \overline{t}$. Then, we can consider the expectation of diagonal element of matrix $\widetilde{\mathbf{C}}_d^{(L)n}$ corresponding to such an antenna position. In fact, this value plays a key role in the performance analysis of linear detectors for such a transmit antenna. Their properties are summarized below.

PROPOSITION 3 *As $L \to +\infty$, the expectation w.r.t. $\widetilde{\Phi}_{\widetilde{\mathcal{A}}_L^\#}^{\widetilde{\mathcal{R}}}$ and $\widetilde{\Phi}_{\widetilde{\mathcal{A}}_L^\#}^{\widetilde{\mathcal{T}}}|t_j = \overline{t}$ of the jth diagonal element of $\widetilde{\mathbf{C}}_d^{(L)n}$ equals $m_{\widetilde{\mathbf{C}}_d}^{(n)}$. More specifically,*

$$\overline{C}^{(1)} = \lim_{L\to+\infty} \mathrm{E}\overline{\boldsymbol{\psi}}_{\widetilde{T}}^{(L)}\widetilde{\mathbf{T}}_d^{(L)}\widetilde{\mathbf{\Psi}}_R^{(L)H}\widetilde{\mathbf{\Psi}}_R^{(L)}\widetilde{\mathbf{T}}_d^{(L)}\overline{\boldsymbol{\psi}}_T^{(L)} = m_{\widetilde{\mathbf{C}}_d}^{(1)}$$

and

$$\begin{aligned}\overline{C}^{(2)} &= \lim_{L\to+\infty} \mathrm{E}\overline{\boldsymbol{\psi}}_T^{(L)}\widetilde{\mathbf{T}}_d^{(L)}\widetilde{\mathbf{\Psi}}_R^{(L)H}\widetilde{\mathbf{F}}_d^{(L)}\widetilde{\mathbf{F}}_d^{(L)H}\widetilde{\mathbf{\Psi}}_R^{(L)}\widetilde{\mathbf{T}}_d^{(L)}\overline{\boldsymbol{\psi}}_T^{(L)} \\ &= m_{\widetilde{\mathbf{C}}_d}^{(2)} \end{aligned} \tag{15}$$

where the expectation is w.r.t. $\Phi_{\widetilde{\mathcal{A}}_L^\#}^{\widetilde{\mathcal{R}}}$ and $\Phi_{\widetilde{\mathcal{A}}_L^\#}^{\widetilde{\mathcal{T}}}|t_j = \overline{t}$ and $\overline{\boldsymbol{\psi}}_T^{(L)} = \left(\frac{1}{\sqrt{(\theta)}}\exp(+\imath\overline{t}\nu/\tau)\right)_{\nu\in\widetilde{\mathcal{L}}_L^\#\setminus\{0\}}$ is a row vector.

In order to obtain an approximate expression of the eigenvalue pdf $f_{\mathbf{C}}(\lambda)$ of matrix $\mathbf{C}$ as $L \to +\infty$ or, equivalently, $N_R, N_T, \theta^2 \to +\infty$ with constant ratios (9) we approximate the matrices $\mathbf{\Psi}_R^{(L)}$ and $\mathbf{\Psi}_T^{(L)}$ by Gaussian matrices of i.i.d. zero mean elements with variance θ^{-2}.

Under this approximation, we obtain the following results.

PROPOSITION 4 *Let $\overline{\mathbf{\Phi}}_T$ and $\overline{\mathbf{\Phi}}_R$ be Gaussian matrices of i.i.d. zero mean elements with variance θ^{-2} and size $\theta^2\times N_T$ and $\theta^2\times N_R$, respectively. Let $\mathbf{A}$ be a $\theta^2\times\theta^2$ diagonal matrix with eigenvalue probability density function that converges to $f_{\mathbf{A}}(x)$, with $x\in\mathbb{R}$, as $\theta^2 \to +\infty$. Then, as θ^2, N_T, $N_R \to +\infty$ with constant ratios $\frac{N_R}{\theta^2}\to\gamma_R$ and $\frac{N_T}{\theta^2}\to\gamma_T$, the asymptotic eigenvalue distribution $f_{\overline{\mathbf{C}}}(x)$ of the matrix*

$$\overline{\mathbf{C}} = \overline{\mathbf{\Phi}}_T\mathbf{A}\overline{\mathbf{\Phi}}_R^H\overline{\mathbf{\Phi}}_R\mathbf{A}\overline{\mathbf{\Phi}}_T^H$$

obeys

$$\begin{aligned} sG_{\overline{\mathbf{C}}}(s)+1 &= -G_{\overline{\mathbf{C}}}(s)\left(\gamma_T sG_{\overline{\mathbf{C}}}(s)+\gamma_T-\gamma_R\right) \\ &\int \frac{x^2 f_{\mathbf{A}}(x)\mathrm{d}x}{1-\gamma_T G_{\overline{\mathbf{C}}}(s)\left(\gamma_T sG_{\overline{\mathbf{C}}}(s)+\gamma_T-\gamma_R\right)x^2} \end{aligned} \tag{16}$$

being $G_{\overline{\mathbf{C}}}(s)$ the Stieltjes transform of $f_{\overline{\mathbf{C}}}(x)$, i.e.

$$G_{\overline{\mathbf{C}}}(s) = \int \frac{f_{\overline{\mathbf{C}}}(x)\mathrm{d}x}{x-s}. \tag{17}$$

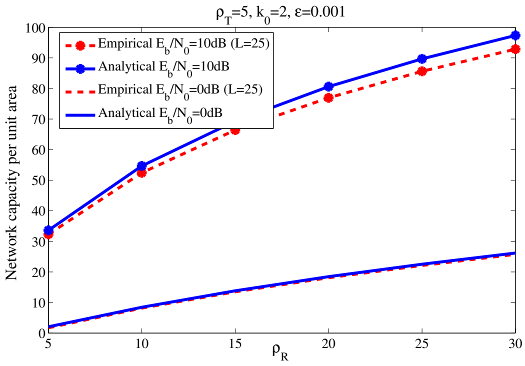

Fig. 2. Capacity per unit area and unit frequency band versus intensity of receive antennas. Intensity of transmit antennas constant $\rho_T = 5$, exponential decaying constant $k_0 = 2$. Solid and dashed lines show the analytical approximation and the actual capacity in a finite network of area $L^2 = 25^5$.

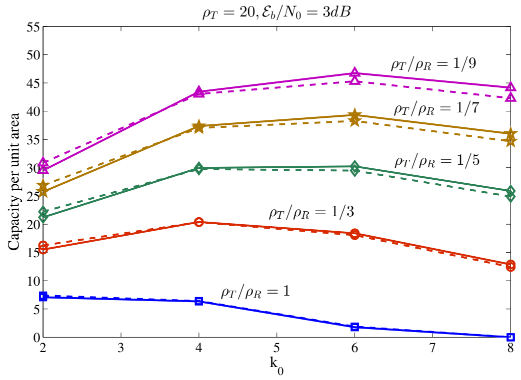

Fig. 3. Capacity per unit area and unit frequency band versus the attenuation coefficient k_0. Intensity of transmit antennas constant $\rho_T = 20$, while the receivers' intensity varies $\rho_R = 20, 60, 100, 140, 180$. Solid and dashed lines show the analytical approximation and the actual capacity in a finite network of area 100, respectively.

The derivation of this result is omitted and follows along the lines of the derivation in [25], Appendix A. Analogous results can be stated for the 1D-system.

IV. Performance Analysis

It is well known that the mathematical tools derived in the previous section are essential to derive the fundamental limits of the system in (4) as the network size grows large. In particular, the total capacity per unit area or throughput of the system is related to the Stieltjes transform provided in Proposition 4 while the eigenvalue moments and the diagonal elements in Proposition 1, 2, and 3 characterize the performance of linear multiuser detectors at a centralized receiver. The first two eigenvalues or the conditional expectations $\overline{C}^{(1)}$ and $\overline{C}^{(2)}$ are sufficient to characterize the performance of the matched filter. We recall here some fundamental relations by referring to the 2D-system. Analogous results can be stated for the 1D-system.

Under the constraint of constant transmit power at the transmit antennas, the capacity per receive antennas in a network over a finite squared box $\mathcal{A}_L^{\#}$ with transfer matrix $\mathbf{F}^{(L)}$ is given by [22]

$$\begin{aligned} C(\rho, \mathbf{F}^{(L)}, N_R, N_T) &= \frac{1}{2N_R} \log_2 \det \left(\mathbf{I} + \rho \mathbf{F}^{(L)} \mathbf{F}^{(L)H} \right) \\ &= \frac{1}{2N_R} \sum_{n=1}^{N_R} \log_2 \left(1 + \rho \lambda_n (\mathbf{F}^{(L)} \mathbf{F}^{(L)H}) \right) \\ &= \frac{1}{2N_R} \sum_{n=1}^{N_T} \log_2 \left(1 + \rho \lambda_n (\mathbf{C}^{(L)}) \right) \end{aligned}$$

being $\rho = \frac{P}{\sigma^2}$ the transmit signal to noise ratio (SNR) and $\lambda_n(\cdot)$ is the n-th eigenvalue of the matrix argument. The average with respect to $\mathbf{F}^{(L)}$ is denoted by

$$C(\rho, N_R, N_T) = \mathrm{E} \left\{ \frac{1}{2N_R} \sum_{n=1}^{N_R} \log_2 \left(1 + \rho \lambda_n (\mathbf{F}^{(L)} \mathbf{F}^{(L)H}) \right) \right\}$$

and the average maximum achievable rate per unit area is

$$\begin{aligned} \mathcal{C}(\rho, N_R, N_T) &= \mathrm{E} \left\{ \frac{1}{2\theta^2 \tau^2} \sum_{n=1}^{N_T} \log_2 \left(1 + \rho \lambda_n (\mathbf{C}^{(L)}) \right) \right\} \\ &= \rho_R C(\rho, N_R, N_T). \end{aligned}$$

Let $\mathcal{E}_b$ be the energy per information bit. Then, when transmitting at total rate $N_R C(\rho, N_R, N_T)$ [21]

$$\begin{aligned} \rho &= \frac{\mathcal{E}_b N_R C(\rho, N_R, N_T)}{\sigma^2 N_T} \\ &= \frac{\mathcal{E}_b \rho_R C(\rho, N_R, N_T)}{\sigma^2 \rho_T} \\ &= \frac{\mathcal{E}_b \mathcal{C}(\rho, N_R, N_T)}{\sigma^2 \rho_T}. \end{aligned}$$

Thus, the average maximum achievable throughput per unit area as a function of $\frac{\mathcal{E}_b}{\mathcal{N}_0} = \frac{\mathcal{E}_b}{\sigma^2}$ is the solution to the fixed point equation

$$\begin{aligned} &\mathcal{C}(\rho, N_R, N_T) = \\ &\quad \mathrm{E} \left\{ \frac{1}{2\theta^2} \sum_{n=1}^{N_T} \log_2 \left(1 + \frac{\mathcal{E}_b \mathcal{C}(\rho, N_R, N_T)}{N_0 \rho_T} \lambda_n (\mathbf{C}^{(L)}) \right) \right\} \end{aligned}$$

As from Proposition 4, when $L \to +\infty$ the eigenvalue distribution of the matrix $\mathbf{C}^{(L)}$ can be approximated by a determinist eigenvalue distribution described by the Stieltjes transform $G_{\overline{\mathbf{C}}}(s)$ in (16). The well known relation between capacity and Stieltjes transform of the eigenvalues of the channel covariance matrix $\mathbf{C}$, (see e.g. [5], [23], [26], [27])

$$\mathcal{C}(\rho) = \frac{\rho_T}{2 \ln 2} \int_0^{\rho} s^{-1} \left(1 - s^{-1} G_{\overline{\mathbf{C}}}(-s^{-1}) \right) \mathrm{d}s$$

provides an approximation of the capacity per unit area as a function of ρ, the SNR.

V. Simulation Results

In this section we compare the capacity per unit area of a 2D-system obtained using the asymptotic analytical approximations with the average capacity obtained by averaging over several network realizations. We consider a system with transmitters homogeneously distributed with intensity $\rho_T = 5$ while the intensity of the receivers varies in the range $\rho_R = [5, 10, 15, 20, 25, 30]$. The coefficient of the exponential pathloss was $k_0 = 2$. In Fig. 2, we show the capacity per unit area when the number of the receivers' intensity increases for $E_b/N_0 = 0$ dB and $E_b/N_0 = 10$ dB. At low values of E_b/N_0 the approximation obtained analytically is very tight while it becomes looser when E_b/N_0 increases. In fact, the approximations made yield a slight mismatch on the tails of the eigenvalue distribution of matrix $\mathbf{C}$. As expected, when the number of receive antennas per unit area increases also the capacity per unit area increases.

Fig. 2 captures the effects of the attenuation on the capacity per unit area. It shows the system capacity versus the attenuation coefficient k_0 for transmitter intensity $\rho_T = 20$ and varying values of the receiver intensity ρ_R. More specifically, $\rho_R = [20,\, 60,\, 100,\, 140\,180]$. As already observed, the capacity per unit area increases when the receiver's intensity increases. However, the channel attenuation is more beneficial for not heavily loaded systems and for load $\rho_T/\rho_R = 1$ the best capacity per unit area is attained when $k_0 = 2$ while for decreasing loads, $\frac{\rho_T}{\rho_R} = \frac{1}{3}, \frac{1}{5}, \frac{1}{7}, \frac{1}{9}$ the best capacity is attained for $k_0 = 4,\, 6,\, 6,\, 6$, respectively. This behavior points out a complex trade off between the number of actually reachable receive antennas from a transmit antenna and the average number of transmit antennas actually served by a receive antennas.

VI. Conclusions

In this contribution we considered a system consisting of distributed transmit and receive antennas randomly distributed over a 1-dimensional and 2-dimensional Euclidean space. The receive antennas are connected to a central receiver and the receive signal is processed jointly. We analyzed the fundamental limits of this system in terms of capacity per unit area. Approximations of the eigenvalue moments to analize the performance of a simple matched filter detector at the receiver when the size of the network grows large are also provided. This analysis is based on the introduction of a new class of ERMs whose entries depend on two independent Bernoulli processes. These matrices capture the effects of the slow fading due to pathloss. Note that the effect of fast fading is neglected in this phase. However, the proposed mathematical framework is capable to capture also the effects of fast fading to some extent. The performance analysis of combined pathloss and Rayleigh fading is left for future studies.

Acknowledgements

This work was supported in part by the European Commission via the 7th framework project HARP and by the French Agence Nationale de la Recherche (ANR) via the International Blanc project IMAGENET.

References

[1] A. A. M. Saleh, A. Rustako, and R. Roman, "Distributed antennas for indoor radio communications," *IEEE Transactions on Communications*, vol. 35, no. 12, pp. 1245–1251, Dec. 1987.

[2] K. Kerpez, "A radio access system with distributed antennas," *IEEE Transactions on Vehicular Technology*, vol. 45, no. 2, pp. 265–275, May 1996.

[3] Y. Lin and W. Yu, "Downlink spectral efficiency of distributed antenna systems under a stochastic model," *Accepted for publication in IEEE Transactions on Wireless Communications*, 2014, on line at http://www.comm.utoronto.ca/ weiyu/publications.html.

[4] J. Gan, Y. Li, L. Xiao, S. Zhou, and J. Wang, "On sum rate and power comsumption of multiuser distributed antenna system with circular antenna layout," *EURASIP Journal on Wireless Communications and Networking*, vol. 2007, Jul. 2007.

[5] R. Couillet and M. Debbah, *Random Matrix Methods for Wireless Communications*. Cambridge University Press, 2011.

[6] W. Feng, Y. Li, S. Zhou, J. Wang, and M. Xia, "Uplink sum capacity evaluation of multi-user distributed antenna systems," *Elsevier, International Journal of Electronics and Communications*, vol. 64, pp. 168–172, Feb. 2010.

[7] L. Dai, "A comparative study on uplink sum capacity with co-located and distributed antennas," *IEEE Journal on Selected Areas in Communications*, vol. 29, no. 6, pp. 1200–1213, Jun. 2011.

[8] B. M. Zaidel, S. Shamai, and S. Verdú, "Multicell uplink spectral efficiency of coded DS-CDMA with random signatures," *IEEE Journal on Selected Areas in Communications*, vol. 19, no. 8, pp. 1556–1569, Aug. 2001.

[9] D. Aktas, M. Bacha, J. Evans, and S. Hanly, "Scaling results on the sum capacity of cellular networks with MIMO links," *IEEE Transactions on Information Theory*, vol. 52, no. 7, pp. 3264 – 3274, july 2006.

[10] N. Levy, O. Zeitouni, and S. Shamai, "On information rates of the fading Wyner cellular model via the Thouless formula for the strip," *Information Theory, IEEE Transactions on*, vol. 56, no. 11, pp. 5495 –5514, nov. 2010.

[11] A. L. Moustakas and N. Bambos, "Power optimization on a random wireless network," in *Proc. of IEEE International Symposium on Information Theory (ISIT)*, Istambul, Turkey, Aug. 2013.

[12] L. Cottatellucci, "Spectral efficiency of extended networks with randomly distributed transmitters and receivers," in *Invited for Proc. of 2nd IEEE China Summit and International Conference on Signal and Information Processing (ChinaSIP14)*, Xi'an, China, Jul. 2014, pp. 673–677.

[13] M. Mézard, G. Parisi, and A. Zee, "Spectra of Euclidean random matrices," *Journal of Physics B: Nuclear Physics*, 1999.

[14] S. E. Skipetrov and A. Goetschy, "Eigenvalue distributions of large Euclidean random matrices for waves in random media," Dec. 2010, arXiv preprint arXiv:1007.1379.

[15] F. Hiai and D. Petz, *The Semicircle Law, Free Random Variables and Entropy*. Providence, RI: American Mathematical Society, 2000.

[16] A. Goetschy and S. Skipetrov, "Non-Hermitian Euclidean random matrix theory," *Phys. Rev. E*, Jun. 2011, arxiv:1102.1850v2.

[17] R. R. Müller, "A random matrix model for communication via antenna arrays," *IEEE Transactions on Information Theory*, vol. 48, no. 9, pp. 2495–2506, Sep. 2002.

[18] L. Cottatellucci and R. R. Müller, "A systematic approach to multistage detectors in multipath fading channels," *IEEE Transactions on Information Theory*, vol. 51, no. 9, pp. 3146–3158, Sep. 2005.

[19] M. Haenggi, *Stochastic Geometry for Wireless Networks*. Cambridge University Press, 2012.

[20] Abdallah and M. Debbah, "Downlink CDMA: to cell or not to cell," in *Proceedings of the 12th European Signal Processing Conference (EUSIPCO'04)*, Vienna, Austria, May 2004.

[21] S. Verdú and S. Shamai (Shitz), "Spectral efficiency of CDMA with random spreading," *IEEE Transactions on Information Theory*, vol. 45, no. 2, pp. 622–640, Mar. 1999.

[22] I. E. Telatar, "Capacity of multi–antenna Gaussian channels," *European Transactions on Telecommunications*, vol. 10, no. 6, pp. 585–595, Nov./Dec. 1999.

[23] S. Shamai (Shitz) and S. Verdú, "The impact of frequency–flat fading on the spectral efficiency of CDMA," *IEEE Transactions on Information Theory*, vol. 47, no. 4, pp. 1302–1327, May 2001.

[24] Ø. Ryan and M. Debbah, "Asymptotic behaviour of random Vandermonde matrices with entries on the unit circle," *IEEE Transactions on Information Theory*, vol. 55, no. 7, pp. 3115–3147, 2009.

[25] R. Müller, L. Cottatellucci, and M. Vehkaperä, "Blind pilot decontamination," *Submitted to IEEE Journal on Selected Areas in Signal Processing*, Sep. 2013, on line: arXiv:1309.6806.

[26] L. Cottatellucci, R. R. Müller, and M. Debbah, "Asynchronous CDMA systems with random spreading–Part I: Fundamental limits," *IEEE Transactions on Information Theory*, vol. 56, no. 4, pp. 1477 – 1497, Apr. 2010.

[27] L. Cottatellucci and M. Debbah, "On the capacity of MIMO Rice channels," in *Proc. 42nd Allerton Conf. on Communication, Control and Computing*, Monticello, Illinois, Sep./Oct. 2004.